



U.S. DEPARTMENT OF
ENERGY

Office of
Science

DOE/SC-CM-21-003

FY 2021 Third Quarter Performance Metric: Enhance and Test Simulations of Sediment and Nutrient Transport from Land to Ocean to Represent Coastal Biogeochemistry

June 2021

DISCLAIMER

This report was prepared as an account of work sponsored by the U.S. Government. Neither the United States nor any agency thereof, nor any of their employees, makes any warranty, express or implied, or assumes any legal liability or responsibility for the accuracy, completeness, or usefulness of any information, apparatus, product, or process disclosed, or represents that its use would not infringe privately owned rights. Reference herein to any specific commercial product, process, or service by trade name, trademark, manufacturer, or otherwise, does not necessarily constitute or imply its endorsement, recommendation, or favoring by the U.S. Government or any agency thereof. The views and opinions of authors expressed herein do not necessarily state or reflect those of the U.S. Government or any agency thereof.

Contents

1.0	Product Definition	1
2.0	Product Documentation	2
3.0	Results	3
3.1	Modeling Soil Erosion	3
3.2	Modeling Sediment Transport.....	6
3.3	Modeling River Nutrient Fluxes	9
3.4	Summary and Future Work.....	12
4.0	References	13

Figures

Figure 1.	Schematic of the framework of modeling sediment and nutrient transport.....	2
Figure 2.	Comparing NRI observations and literature estimates of cropland soil erosion (a), sediment yield (b), and POC yield (c) with ELM-Erosion estimates.	5
Figure 3.	ELM-Erosion simulated sediment yields to inland waters in the 0.125° NLDAS domain.	5
Figure 4.	A new national map of median sediment particle diameter (D50) for river beds.....	6
Figure 5.	Simulated versus observed annual mean discharge of water (gold) and suspended sediment (blue) (including both mud and sand).....	7
Figure 6.	Impacts of reservoirs on (a) water and (b) suspended sediment discharge to the coasts.	9
Figure 7.	(a) Map of the large river basins and USGS 2-digit Hydrologic Units (HUCs) in the CONUS selected for model validation and analysis and (b) comparison of simulated eroded organic matter C/N ratios (diamonds) with previously estimated C/N ratios of suspended organic matter (circles).	10
Figure 8.	Comparing the modeled (blue) and observed (red) PP yields in the six large rivers of the Mississippi river basin during the water year of 1992–2018.	11
Figure 9.	Increased extreme rains in the Mississippi river basin intensify erosional nutrient fluxes.	12

1.0 Product Definition

Coastal zones, a tiny portion of the land-ocean continuum, are hotspots for ecological and socioeconomic activities. Coastal ecosystem dynamics are primarily controlled by coastal biogeochemistry, which is subject to the strong influences of terrestrial sediment and nutrient fluxes transported by rivers. For example, excess nutrient discharge from the Mississippi River has been a primary cause of the recurring hypoxic dead zone in the Gulf of Mexico (Rabalais et al. 2002, Turner et al. 2008, McLellan et al. 2015, Feng et al. 2019). In 2017, this hypoxic zone reached the size of 22,720 km², the largest ever measured and as big as the entire state of New Jersey (Van Meter et al. 2018). Moreover, coastal carbon cycling is largely regulated by terrestrial sediment and nutrient fluxes due to the close physical and chemical interactions between various carbon elements and sediment and nutrient substances (Zaehle et al. 2011, Browning et al. 2017). Last but not least, the decline of territorial sediment flux is one of the major reasons for the shifting coastline in the past decades (Valderrama-Landeros et al. 2019, Warrick et al. 2019).

Sediment and nutrient transport from land to the ocean via rivers is generally lacking or underrepresented in Earth System models (ESMs) because ESMs lack physically based representation of riverine hydraulic and thermodynamic conditions critical for representing the transport and transformation of riverine sediment and nutrient fluxes. The riverine component of Energy Exascale Earth System Model (E3SM), Model for Scale Adaptive River Transport (MOSART), has been well tested and validated for simulating riverine hydraulic and thermodynamic processes in both natural and managed river systems (Li et al. 2013, 2015a, b, Voisin et al. 2013a, b, Yigzaw et al. 2018, 2019). In particular, MOSART incorporates reservoir regulation and thermal stratification processes that have significant effects on riverine hydraulic and thermodynamic conditions and, consequently, on riverine sediment and nutrient fluxes. Therefore E3SM has unique capabilities to represent sediment and nutrient fluxes from land to the ocean for modeling coastal biogeochemistry under climate and other human-induced changes.

This metric report summarizes recent efforts supported by the U.S. Department of Energy (DOE) in developing and evaluating new coastal modeling capabilities in E3SM including: (1) a process-based soil erosion model within the E3SM land model (ELM), ELM-Erosion, to simulate sediment yield from land surface to rivers (Tan et al. 2017, 2018), (2) a physically based riverine suspended sediment transport module within MOSART, MOSART-sediment (Li et al. in prep), together with a newly developed median sediment particle size map over the contiguous United States (CONUS) (Abeshu et al. in prep), and (3) a module to simulate erosional carbon, nitrogen, and phosphorus fluxes from land to rivers and coast, highlighting the significant role of extreme rainfall (Tan et al. 2020, 2021). These modules have been successfully validated against observations in the contiguous U.S., demonstrating the ability of E3SM in simulating soil erosion and hillslope sediment yield in CONUS and reproducing the observed long-term suspended sediment discharge in a number of U.S. Geological Survey (USGS) stations. The development of these components fills a key gap in coastal modeling and provides the foundation for further development in representing coastal biogeochemistry in E3SM.

2.0 Product Documentation

The overall framework of modeling sediment and nutrient transport in E3SM is summarized in Figure 1. This document describes the development and testing of key components, including ELM-Erosion, MOSART-sediment, and erosional carbon (C), nitrogen (N), and phosphorus (P) fluxes, representing processes shown by the solid lines, while ongoing and future development focuses on processes shown by the dashed lines.

ELM-Erosion is an event-scale soil erosion model developed based on the improved Morgan-Morgan-Finney (MMF) soil erosion scheme (Tan et al. 2018). It simplifies the complex water erosion processes into rainfall-driven and runoff-driven erosion and defines hillslope sediment flux as the sum of the two erosional fluxes, capped by the sediment transport capacity (solid pink arrow in Figure 1 marked “hillslope routing” from ELM to MOSART). Soil erosion and sediment transport capacity in ELM-Erosion are represented as functions of E3SM simulated hydrological conditions (i.e., direct throughfall, leaf drainage, and surface runoff), vegetation conditions (i.e., plant leaf area index and canopy height), and soil texture, land slope, and land use. Hillslope fluxes of particulate organic carbon (POC), particulate nitrogen (PN), and particulate phosphorus (PP) are also represented in ELM-Erosion (solid dark green arrow in Figure 1 marked “hillslope routing” from ELM to MOSART), based on the modeled sediment flux and the E3SM-simulated surface soil organic C, solid-form N, and solid-form P content, and soil C, N, and P pools are updated based on the simulated POC, PN, and PP fluxes (Tan et al. 2020, 2021).

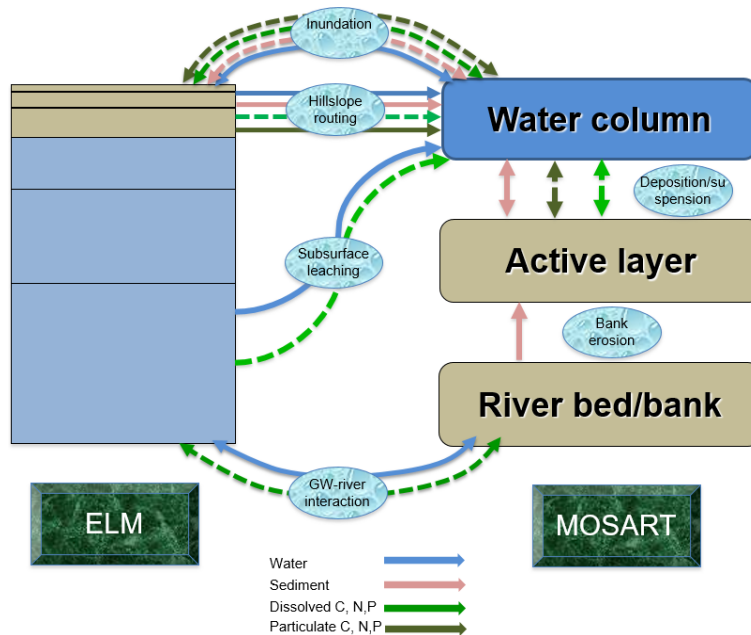


Figure 1. Schematic of the framework of modeling sediment and nutrient transport. Processes that are represented by modules described in this report and processes that will be represented by ongoing/planned efforts are indicated by solid and dashed lines, respectively. The direction of arrows indicates which model is receiving the fluxes simulated by the other model (e.g., ELM-->MOSART means the flux is simulated by ELM and sent to MOSART). ELM-Erosion simulates hillslope sediment flux (solid pink arrow marked “hillslope routing”) and hillslope particulate C and nutrient fluxes (solid dark green arrow marked “hillslope routing”) that are sent to MOSART. MOSART-sediment simulates river sediment dynamics (solid pink arrows marked “deposition/suspension” and “bank erosion”).

MOSART-sediment is a river sediment dynamics model developed on top of the MOSART river routing model and water management (WM) model. As illustrated in Figure 1 (solid pink arrows within MOSART), MOSART-sediment receives hillslope sediment flux calculated by ELM-Erosion and routes it through river channels as mud sediment (median diameter ≤ 0.0625 mm) that is assumed to be well mixed with water and not deposited on the channel bed. MOSART-sediment also simulates the transport of fine sand sediment ($0.0625 < \text{median diameter} \leq 0.25$ mm), which is assumed to be produced only from channel erosion and is frequently exchanged with the material in the channel bed and in-channel bars and controlled by the local hydrodynamical and grain size conditions (Figure 1). The effects of reservoirs on suspended sediment, including the trapping of suspended sediment within the reservoirs and the regulation of the hydraulic conditions controlling the suspended sediment transport, are also explicitly represented in MOSART sediment through coupling between MOSART and WM. ELM-Erosion has been incorporated in E3SM v2 and MOSART-sediment will be released with E3SM v3. Enhancement of ELM-Erosion for the cropland management effect on soil erosion is ongoing and planned for release with E3SM v3. For MOSART, sediment deposition on floodplains and the transport and reactions of river POC and dissolved organic C (DOC) are being developed under the E3SM and Integrated Coastal Modeling (ICoM) projects.

Both ELM-Erosion and MOSART-sediment have been validated over CONUS using Phase 2 of the North American Land Data Assimilation System (NLDAS-2) atmospheric forcing data and the 0.125° NLDAS grid configuration. The model evaluation focused on the Mississippi river basin that contributes the most sediment, C, and nutrient fluxes to the U.S. coastal waters. Model parameters of soil erosion and hillslope sediment and POC fluxes were calibrated based on sensitivity experiments for 1991–2012. The simulated soil erosion and hillslope sediment and POC fluxes were compared with the U.S. Department of Agriculture (USDA) National Resources Inventory (NRI) state-level soil erosion estimate and the pre-dam river sediment and POC yield data in large U.S. river basins, respectively. The hillslope PN and PP fluxes simulated by ELM-Erosion from 1991 to 2019 were used as input to an empirical nutrient spiraling model to estimate river PN and PP yields to oceans (Tan et al. 2021). The simulated C/N and C/P ratios in river-suspended particles and the amount of river PN and PP yields in large U.S. river basins were compared with published and USGS data.

Coupled with ELM, MOSART was run from 1991 to 2012 using the diffusive wave routing method and a new median sediment particle size map to evaluate the simulated streamflow and suspended sediment against measurements at 63 USGS river gauges with at least five years of daily records (Li et al. in review). In addition, three representative USGS gauges (one in the Missouri River and two in the Mississippi River) were selected to evaluate the effect of reservoir operation on suspended sediment. Three MOSART-sediment simulations were performed to isolate the net effects of reservoir regulation and trapping on suspended sediment transport. To represent the effects of reservoir operations, the locations of 1839 relatively large reservoirs (storage capacity ≥ 0.1 km³) were extracted from the GRand database.

3.0 Results

3.1 Modeling Soil Erosion

As soil erosion alters the soil C, N, and P pools, long spin-up simulations were performed to establish the C, N, and P pools before simulations were performed for model evaluation. The ELM land C

biogeochemistry was first spun up for 200 years with accelerated decomposition spin-up, followed by another 600 years with regular spin-up, by recycling the atmospheric forcing from an E3SM preindustrial simulation (Golaz et al. 2019). After the total ecosystem C reached an equilibrium, ELM was run from 1850 to 1990 using atmospheric forcing from an E3SM historical simulation to generate initial conditions for the land states.

To test how well ELM-Erosion represents the spatial variability of soil erosion and hillslope sediment and POC fluxes, we conducted a parameter sensitivity experiment of ELM-Erosion in which an ensemble of 1200 model simulations with 1200 randomly sampled values of the three model parameters were run from 1991 to 2012. The parameter sensitivity experiment shows consistency of the model state-level estimates with the NRI benchmark data (Figure 2a). Erodible soils, vast cropland areas, and relatively frequent precipitation all contribute to high soil erosion in the Midwest and large sediment and POC loadings to inland waters in the Mississippi river basin (Figure 3). The estimates of hillslope sediment and POC fluxes to the Mississippi river basin are as large as 400 Tg/yr and 9 Tg C/yr, respectively. In contrast, due to the flat topography and sparse agricultural activities, the Saint Lawrence river basin delivers very low quantities of sediment and POC (5 Tg/yr and 0.2 Tg C/yr, respectively) to inland waters. ELM-Erosion shows a smaller negative bias in modeling hillslope sediment flux over the USGS hydrologic units dominated by small river basins (e.g., NE Atlantic, SE Atlantic, and SW Pacific) than the benchmark model of Cohen et al. (2013) (Figure 2b). Notably, estimates of soil erosion and pre-dam sediment and POC yield from literature mostly fall between the 25th and 75th percentile estimates of ELM-Erosion (Figure 2), indicating that even the uncalibrated ELM-Erosion can reproduce the spatial variability of soil erosion in CONUS quite well.

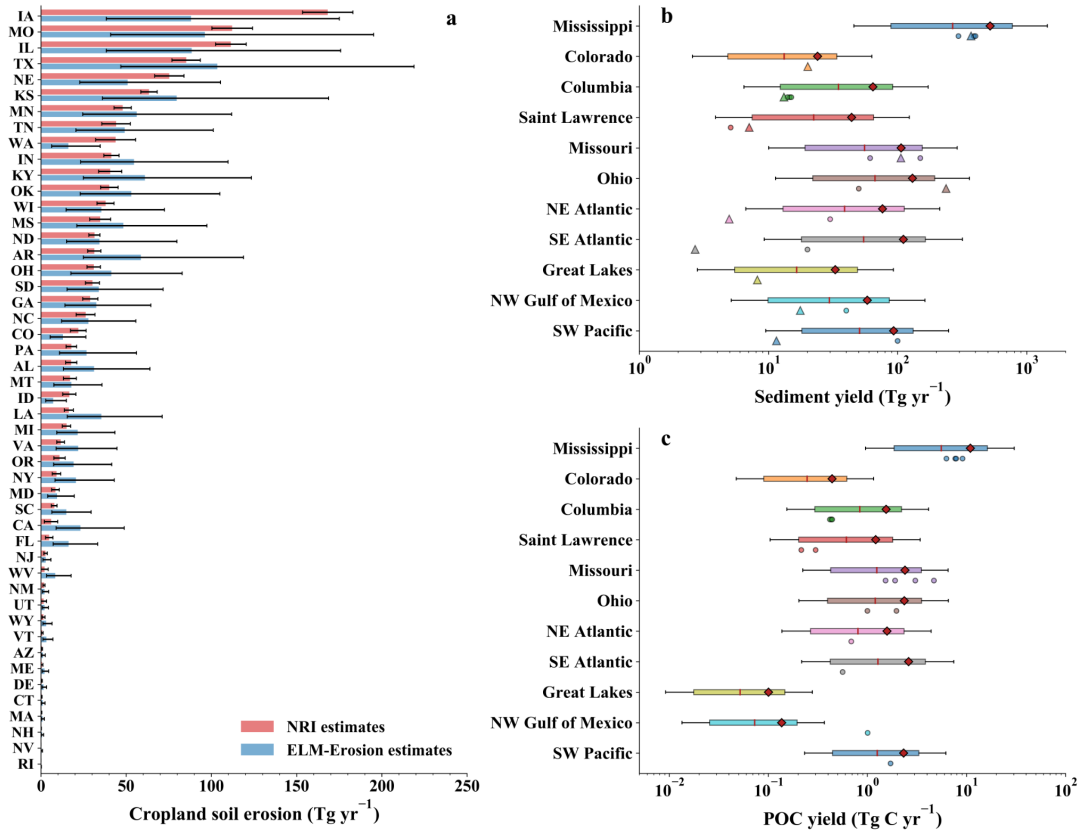


Figure 2. Comparing NRI observations and literature estimates of cropland soil erosion (a), sediment yield (b), and POC yield (c) with ELM-Erosion estimates. In (a), the bars represent the mean and standard deviation of the NRI benchmark estimates and the median, 25th percentile, and 75th percentile values of the ELM-Erosion estimates. The box plots of ELM-Erosion estimates in (b) and (c) represent the median (red line), mean (red star), 10th percentile (left whisker), 25th percentile (left box edge), 75th percentile (right box edge), and 90th percentile (right whisker) values. Observations and literature benchmark estimates in (b) and (c) are represented by circles and triangles, respectively.

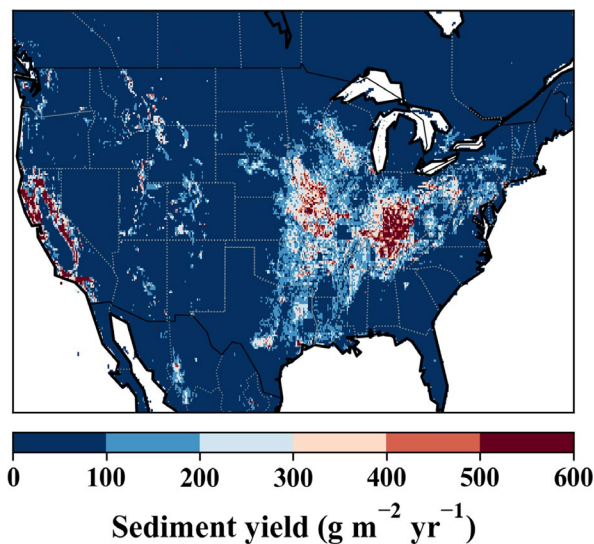


Figure 3. ELM-Erosion simulated sediment yields to inland waters in the 0.125° NLDAS domain.

3.2 Modeling Sediment Transport

Sediment transport depends critically on the sediment particle size in river beds. To support large-scale modeling of sediment transport, a new national map of median sediment particle size (D50) in river beds was developed to provide estimates of the most critical parameter (D50) for riverine sediment modeling. Numerical experiments were performed using MOSART-sediment for comparison with observations. These two tasks are briefly summarized below.

Despite the importance of bed-material sediment particle size, such data has limited availability due to the expensive costs of measuring and analyzing them. As one of the most data-rich countries in the world, the United States collects and disseminates the sediment particle size data mainly through two federal agencies: The USGS and the U.S. Army Corps of Engineers (USACE). USGS manages the most gauges and distributes the river-related measurements on the U.S. rivers. As of April 2021, there are 424,948 stations with field/laboratory samples in the USGS water quality portal, among which 1.2% (4,991) include bed-material sediment particle data for rivers over the contiguous U.S., and 0.5% (2,277) have complete percentiles of bed-material sediment particle data to compute D50.

To overcome the limited sampling of D50 to support modeling of sediment transport, a map of D50 was developed over CONUS in a vector format that corresponds to millions of river segments in the National Hydrography Dataset Plus (NHDplus) data set, as shown in Figure 4 (Abeshu et al. in prep). The map development involves four steps: 1) collect and process the observed D50 data from 2,577 USGS stations or USACE sampling locations; 2) collocate these data with the NHDplus flowlines based on their geographic locations, resulting in 1,691 flowlines with collocated D50 values; 3) develop a predictive model using the eXtreme Gradient Boosting (XGBoost) machine learning method trained on the observed D50 data and the corresponding climate, hydrology, geology, and other attributes retrieved from the NHDplus data set; 4) estimate the D50 values for flowlines without observations using the XGBoost predictive model.

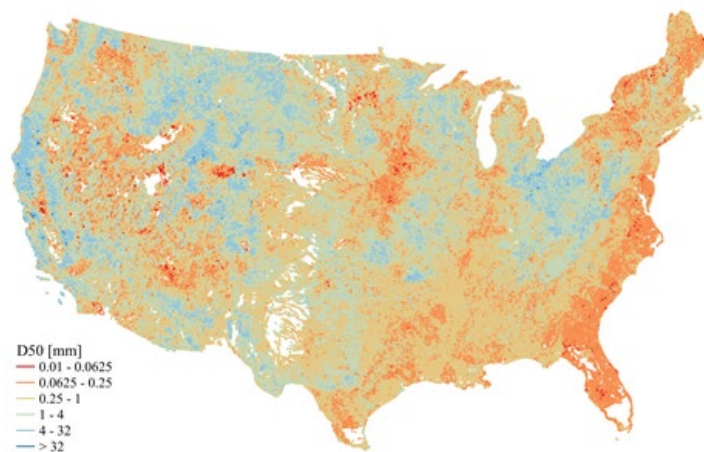


Figure 4. A new national map of median sediment particle diameter (D50) for river beds.

We applied MOSART-sediment over CONUS at an hourly time step and 1/8th-degree spatial resolution in the period 1979–2012. The D50 map in Figure 4 is converted from vector format to grid-based format at the 1/8th-degree spatial resolution consistent with the other MOSART parameters. The Manning’s roughness coefficient values for hillslope and channel routing were estimated based on

the land-use and hydraulic conditions. Values of all other model parameters were prescribed based on values used in previous MOSART applications over CONUS. To isolate the net effects of reservoir regulation and trapping on suspended sediment transport, three numerical simulations were performed: (1) **sim_nat**, with MOSART-sediment configured under natural river conditions with no reservoir regulation or trapping; (2) **sim_wm_only**, with MOSART-sediment configured with the water management option, but reservoir trapping was turned off; (3) **sim_wm_trapping**, with MOSART-sediment configured with the water management option to include both flow regulation and reservoir trapping effects. The individual effects of reservoir regulation and trapping can be estimated by comparing **sim_nat** with **sim_wm_only** and comparing **sim_wm_only** and **sim_wm_trapping**, respectively. Each simulation was driven by the same sediment yield time series for the period of 1979–2012 provided by ELM-soil-erosion. Parameter calibration was not conducted for the riverine component. The period of 1979–1990 was used for model spin-up, and the simulation results for 1991–2012 were analyzed for model validation.

MOSART-sediment reasonably well captured the long-term average suspended sediment discharge values across CONUS, as shown by the comparison between the simulated (**sim_wm_trapping**) and observed long-term averaged values at multiple USGS gauges (Figure 5). The discrepancy between the simulated and observed average sediment discharges appears to be larger at USGS gauges with smaller upstream drainage areas, which can partly be attributed to the difference between the simulated and observed average water discharges. Another source of model biases is uncertainties in the parameters affecting the riverine hydraulic conditions and sediment transport capacity, such as channel bed slope, Manning’s roughness, channel geometry, etc.

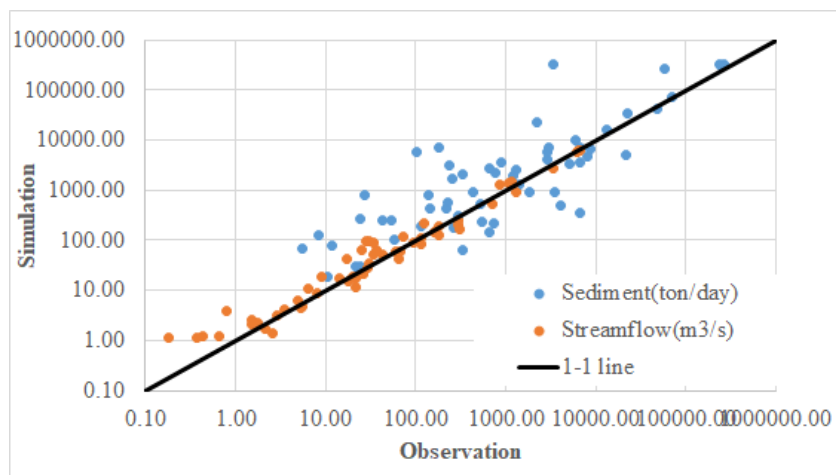


Figure 5. Simulated versus observed annual mean discharge of water (gold) and suspended sediment (blue) (including both mud and sand). The simulation here used is **sim_wm_trapping**.

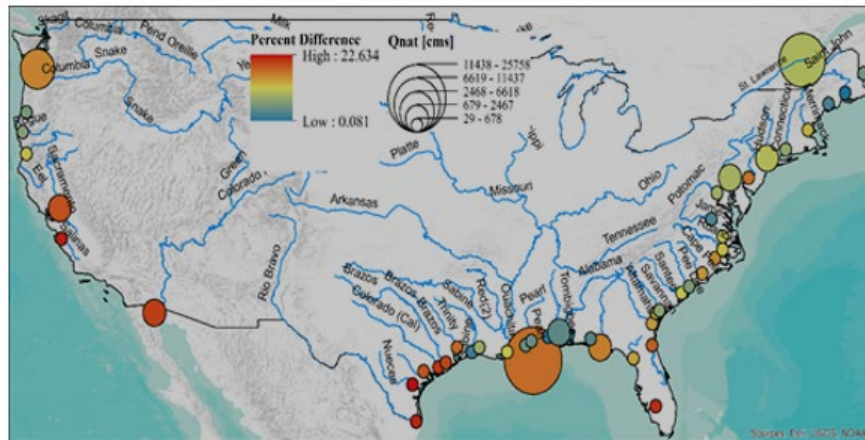
Most of the river systems eventually deliver fresh water and suspended sediment discharges to the coasts. Figure 6 shows the simulated impacts of water management on freshwater discharge and the impacts of reservoirs on suspended sediment discharge to the coasts. Each dot in Figure 6 represents the river mouth of a river system. The larger the dot size, the larger the freshwater or suspended sediment discharge without reservoirs (i.e., under natural river conditions). The color of each dot represents the percentage of natural freshwater or suspended sediment discharge that is reduced by water management or reservoirs. According to our simulations, water management reduces the freshwater discharge to the coasts, particularly for the smaller managed rivers along the southern coasts, as shown in Figure 6a. The

portion of streamflow reduction is relatively smaller in large rivers. The major cause of reduction in freshwater discharge is surface water extraction (which is mainly controlled by water demand intensity). Reservoir regulation normally only changes the seasonal variations of streamflow but does not reduce streamflow on a decadal or longer scale (e.g., in the period 1991–2012).

The delivery of suspended sediment from the continental U.S. to the coasts is largely reduced by the reservoirs, particularly over the large river systems that are strongly influenced by multiple large reservoirs, as shown in Figure 6b. According to our simulation results, the reduction of suspended sediment discharge by reservoirs is high (e.g., over 95%) in some river basins such as the Colorado River and Brazos River but medium or low in other rivers such as the Mississippi and Columbia. These rivers have a large proportion of mud relative to the total sediment discharge. As such, sediment trapping by the reservoirs plays a vital role in retaining mud. For many small rivers close to the coasts, most of the suspended sediment discharge is delivered to the coasts without being trapped during transport. We do not find any notable relationship between the percentage reductions in streamflow with those in suspended sediment discharge at the mouths of rivers. For the former, surface water extraction is the major cause, while for the latter, reservoir trapping is the major cause. These two major causes do not directly interact with each other, suggesting that the reduction of suspended sediment discharge may not be closely linked to the reduction of streamflow. Further investigations using more comprehensive observational data sets and modeling approaches are needed to confirm and improve this finding.

Last but not least, our estimates of suspended sediment discharge from large rivers to the coasts are comparable with previously reported numbers. Within the conterminous United States, the greatest amount of sediment is transported by rivers within the Gulf of Mexico drainage system. Meade and Moody (2010) reported that in 1987–2003, the Mississippi River system on average discharged 172 million tons/year to the coast, which is lower than our estimation of 256 million-tons/year from **sim_wm_trapping** (used in all comparisons discussed below unless stated otherwise). For the Brazos River, one of the largest rivers after the Mississippi River in terms of sediment load delivered to the Gulf of Mexico, Curtis et al. (1973) estimated 32 million tons/year. Ten years later, Milliman and Meade (1983) estimated it to be 16 million tons/year, a much-reduced value. Our estimate is 1.7 million tons/year, even further reduced, which is not unreasonable given the decreasing trend of suspended sediment discharge in the U.S. river systems over the past few decades due to improved soil erosion controls (Meade and Moody 2010). In the current study, however, MOSART-sediment does not account for the coast-river interactions, e.g., tidal effects to the rivers upstream of the outlets. Therefore the estimated sediment discharge to the coasts may contain large uncertainty and should be interpreted with caution.

a. Impacts of water management on streamflow to the coasts.



b. Impacts of reservoirs on suspended sediment discharge to the coasts.

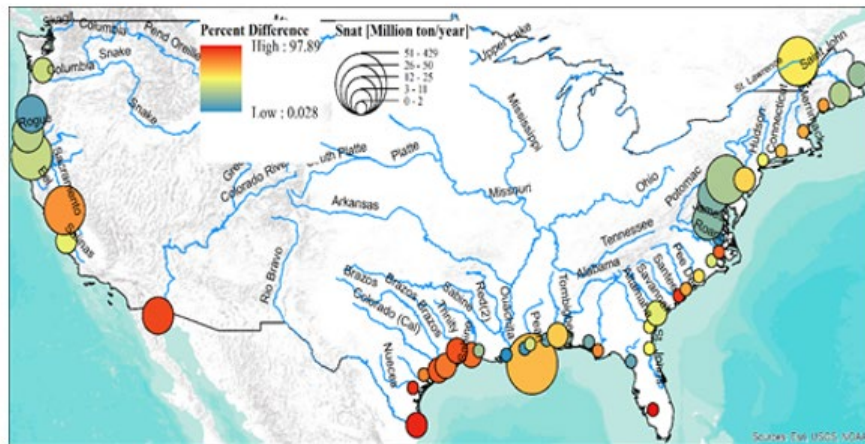


Figure 6. Impacts of reservoirs on (a) water and (b) suspended sediment discharge to the coasts. The size of the circles represents the streamflow and sediment discharge in the simulation with natural conditions (sim_nat). The percent difference shown by the colors is calculated as $(\text{sim_nat} - \text{Sim_wm_trapping})/\text{sim_nat}$.

3.3 Modeling River Nutrient Fluxes

Climate and anthropogenic disturbance such as land use and cropland management have important influences on soil erosion and erosional nutrient fluxes. To understand their relative contributions to the observed changes of river nutrient fluxes to the U.S. coasts, we performed three simulations: (1) simulation $S0$ with land-use change and cropland management actions; (2) simulation $S1$ with fixed land use and no cropland management actions; and (3) simulation $S2$ with the same settings as $S0$ except that non-extreme rainfall in the NLDAS forcing was detrended (Tan et al. 2021). In $S0$ and $S2$, land-use data was extracted from the Land Use Harmonized version 2 (LUH2) transient data set. The effect of cropland management actions on soil erosion was extracted from the state-level cropland soil erosion intensity estimate in the USDA NRI benchmark data.

Model validation shows that ELM-Erosion can reproduce the C/N ratios of suspended sediment in the large CONUS rivers (Figure 7). Realistic simulation of the spatial variability of POC fluxes and C/N

ratios (Figure 2c) indicates that ELM-Erosion is able to reproduce the spatial variability of PN fluxes. In most cases, the estimated C/N ratios have relative errors less than 10%. The simulated C/P ratios of suspended sediment are very close to 22 across CONUS, which is consistent with the documented values from literature (Meybeck 1982). Using an empirical nutrient spiraling method, we reproduced the interannual variability of riverine PP yields at the outlets of large rivers in the Mississippi river basin (Figure 8). Both model estimates and observations show that the riverine PP yield in the Mississippi river basin increased during the water year of 1992–2018: the observed trend is 1.3 Gg P/yr (Mann-Kendall test, $p < 0.05$) and the estimated trend is 1.7 Gg P/yr (Mann-Kendall test, $p < 0.05$). Results of $S0$ show that soil erosion transports enormous amounts of PN and PP from land to rivers in CONUS during 1991–2019: on average 1047 ± 269 Gg N/yr and 445 ± 215 Gg P/yr, respectively. The Mississippi river basin has the largest erosional PN and PP fluxes in CONUS: 718 ± 102 Gg N/yr and 302 ± 105 Gg P/yr, respectively. This basin also contributes nearly 90% of PN and PP yields to the northern Gulf of Mexico. Compared with $S0$, erosional PN and PP fluxes in CONUS in $S1$ are only on average 70 Gg N/yr and 29 Gg P/yr higher, respectively. The small difference between $S0$ and $S1$ can be explained by the gradual maturity of cropland management actions and the minor change of land use in the U.S. since the 1990s. It also indicates that climate change is the major driver of the observed PP yield increase in recent decades. But without cropland management actions and reforestation efforts, erosional PN and PP would have increased more quickly in CONUS during 1991–2019.

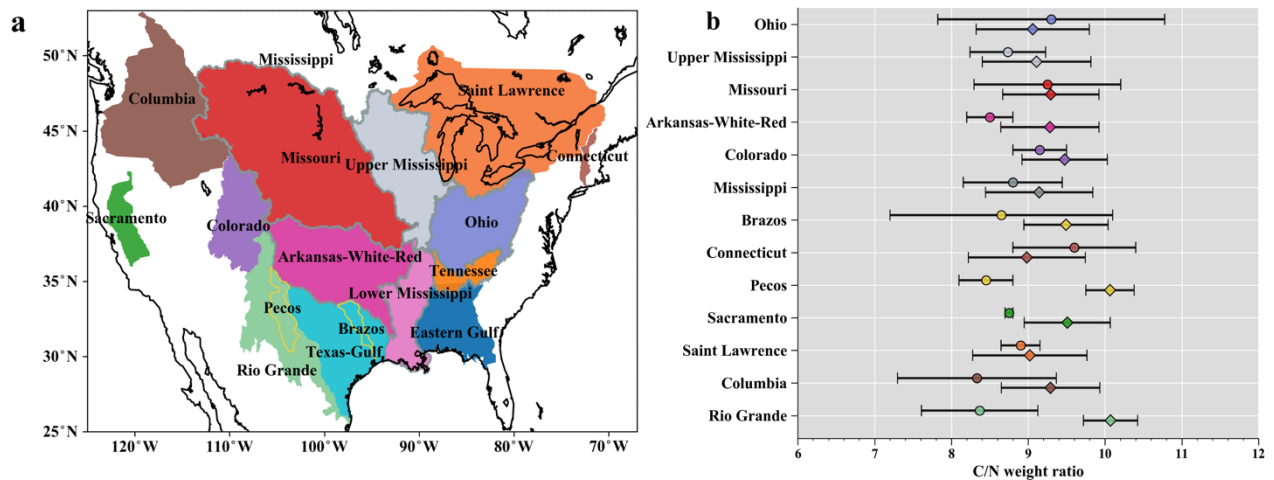


Figure 7. (a) Map of the large river basins and USGS 2-digit Hydrologic Units (HUCs) in the CONUS selected for model validation and analysis and (b) comparison of simulated eroded organic matter C/N ratios (diamonds) with previously estimated C/N ratios of suspended organic matter (circles). The Mississippi/Atchafalaya river basins are outlined with grey boundaries.

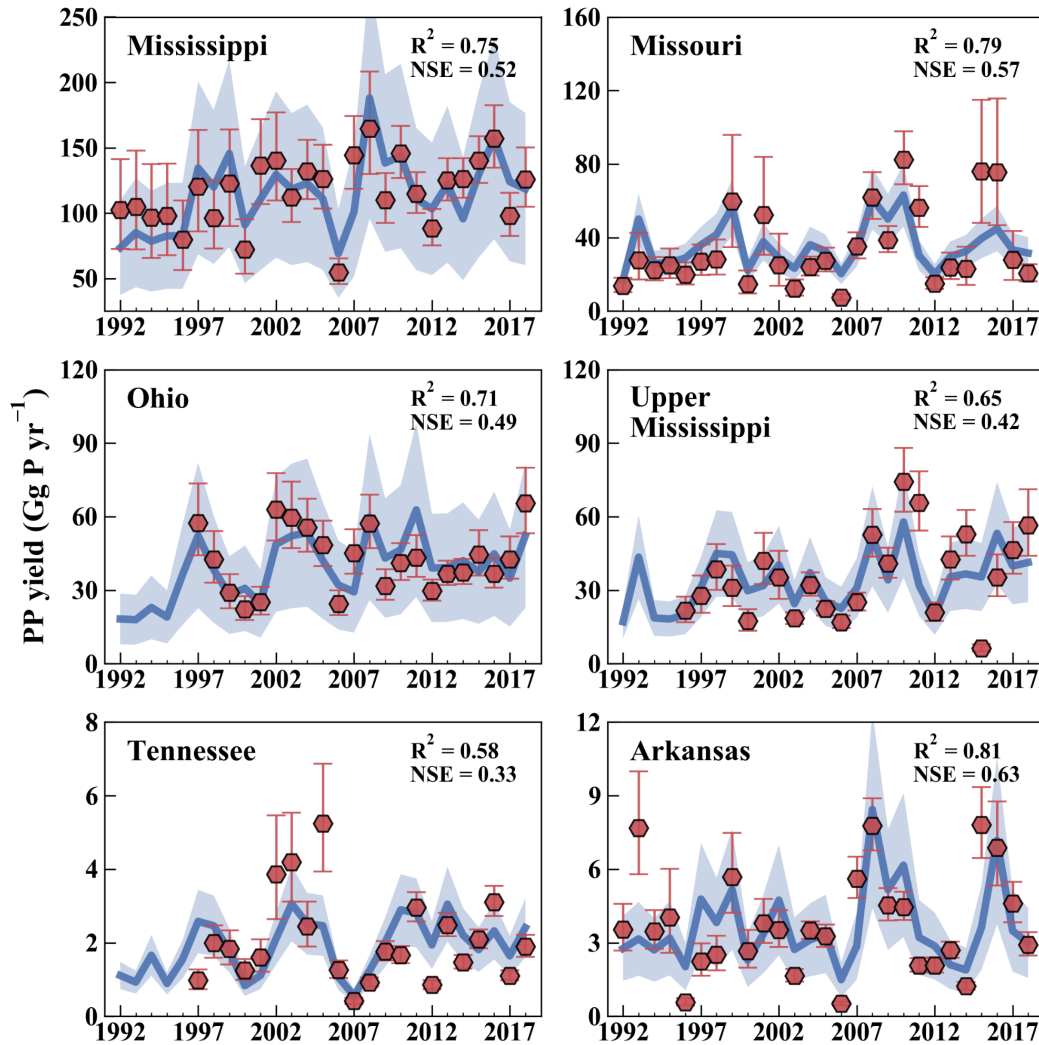


Figure 8. Comparing the modeled (blue) and observed (red) PP yields in the six large rivers of the Mississippi river basin during the water year of 1992–2018. Blue lines and shaded areas represent the mean and the 5th and 95th percentiles of the modeled PP yields based on S_0 . Red hexagons and error bars represent the mean and the 5th and 95th percentiles of the observed PP yields. NSE is the Nash–Sutcliffe efficiency (NSE).

Our analysis further shows that the positive trend of riverine PN and PP yields are mainly caused by the increased erosional PN and PP fluxes in Ohio, Tennessee, and Upper Mississippi river basins (Figure 9). Compared with erosional PN and PP fluxes during days with mild rains, those during days with extreme rain events contribute as much as 80% of the positive trend (Figure 9). This is because the mean annual rainfall and runoff in the regions only increased mildly but even a mild increase of extreme rains can cause a much larger increase of runoff extremes, which would generate a lot of soil erosion and sediment flux.

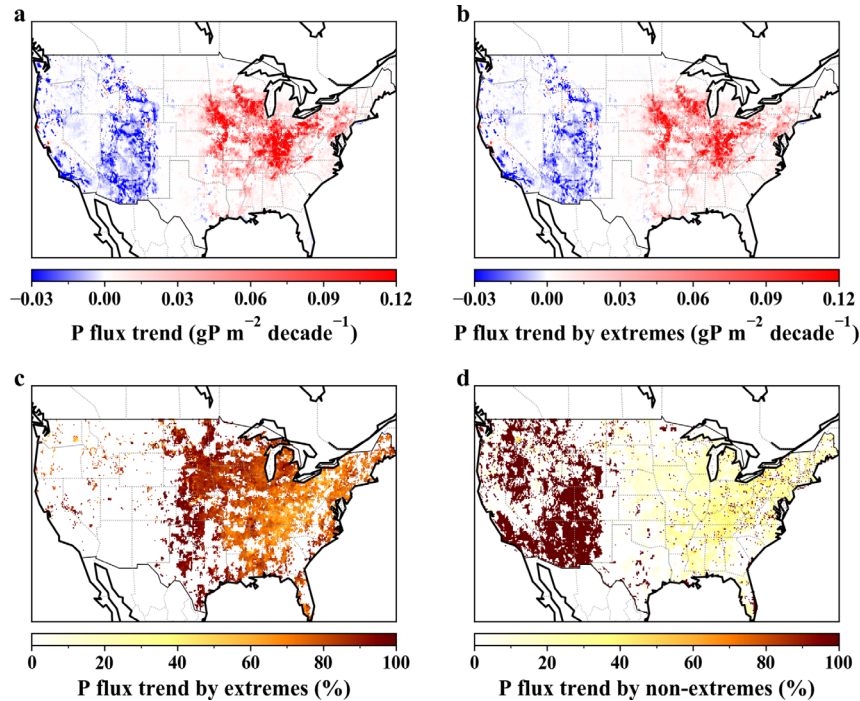


Figure 9. Increased extreme rains in the Mississippi river basin intensify erosional nutrient fluxes. (a)-(b) show the phosphorus flux trend caused by the change of total and extreme rainfall, respectively, with clear increases (red) shown for the eastern U.S. (c)-(d) show the relative contribution of extreme and non-extreme rainfall to the phosphorus flux trend, with flux in the eastern U.S. strongly dominated by extreme rainfall.

3.4 Summary and Future Work

In summary, three modules in ELM and MOSART have been developed to simulate soil erosion, suspended sediment, and particulate C, N, and P from land to oceans via rivers. These modules have been successfully validated against observations in the contiguous U.S. ELM-Erosion is able to capture the spatial variability of soil erosion and hillslope sediment yield in CONUS. It also well predicts the control of climate and land-use change on hillslope fluxes of sediment, N, and P fluxes to river networks. MOSART-sediment reproduces reasonably well the observed long-term suspended sediment discharge in a number of USGS stations, and including reservoir trapping significantly improves sediment discharge simulation with large impacts on sediment load to the coast. These new capacities provide a solid foundation for improving the estimation of terrestrial inputs to coastal biogeochemistry.

Under the E3SM and ICoM projects, several new modules are being developed, including: 1) ELM-MOSART-Carbon, which includes the lateral leaching of POC and DOC from ELM to MOSART and riverine C transport and reaction processes; 2) MOSART-lake, which accounts for the fluxes between lakes and rivers, dynamic variations of lake surface area and volume with lake water depth, and more realistic exchanges between lake surface and atmosphere; 3) MOSART-inundation-sediment, which allows sediment exchanges between river channels and floodplains; 4) enhancement of ELM-Erosion for the cropland management effect on soil erosion. In the near future, development of several important modules is also being planned to facilitate coastal biogeochemistry modeling within E3SM in a closely coupled fashion, including but not limited to: 1) ELM-MOSART-Nitrogen includes the lateral leaching of

particulate and dissolved N and its riverine processes; 2) ELM-MOSART-Phosphorous includes the lateral leaching of particulate and dissolved P and its riverine processes.

4.0 References

Abeshu, GW, H-Y Li, Z Zhu, Z Tan, and LR Leung. 2021. “Median Bed-Material Sediment Particle Size across Rivers in the Contiguous U.S.” *Earth System Science Data*, in prep.

Browning, TJ, EP Achterberg, I Rapp, A Engel, EM Bertrand, A Tagliabue, and CM Moore. 2017. “Nutrient co-limitation at the boundary of an oceanic gyre.” *Nature* 551: 242–246, <https://doi.org/10.1038/nature24063>

Cohen, S, AJ Kettner, JP Syvitski, and BM Fekete. 2013. “WBMsed, a distributed global-scale riverine sediment flux model: Model description and validation.” *Computers & Geosciences* 53: 80–93, <https://doi.org/10.1016/j.cageo.2011.08.011>

Curtis, WF, JK Culbertson, and EB Chase. 1973. Fluvial-sediment discharge to the oceans from the conterminous United States. U.S. Geological Survey. [Circular 670](#), 17p.

Feng, Y, SF DiMarco, K Balaguru, and HJ Xue. 2019. “Seasonal and Interannual Variability of Areal Extent of the Gulf of Mexico Hypoxia from a Coupled Physical-Biogeochemical Model: A New Implication for Management Practice.” *Journal of Geophysical Research – Biogeosciences* 124(7): 1939–1960, <https://doi.org/10.1029/2018JG004745>

Li, H, M. S Wigmosta, H Wu, M Huang, Y Ke, AM Coleman, and LR Leung. 2013. “A physically based runoff routing model for land surface and earth system models.” *Journal of Hydrometeorology* 14(3): 808–828, <https://doi.org/10.1175/JHM-D-12-015.1>

Li, H-Y, LR Leung, T Tesfa, N Voisin, M Hejazi, L Liu, Y Liu, J Rice, H Wu, and X Yang. 2015a. “Modeling stream temperature in the Anthropocene – An earth system modeling approach.” *Journal of Advances in Modeling Earth Systems* 7(4): 1661–1679, <https://doi.org/10.1002/2015MS000471>

Li, H, LR Leung, A Getirana, M Huang, H Wu, Y Xu, J Guo, and N Voisin. 2015b. “Evaluating global streamflow simulations by a physically based routing model coupled with the community land model.” *Journal of Hydrometeorology* 16(2): 948–971, <https://doi.org/10.1175/JHM-D-14-0079.1>

Li, H-Y, Z Tan, H Ma, S Zhu, G Abeshu, T Zhou, JG Duan, and LR Leung. 2021. “Representing Suspended Sediment in Earth System Models.” *Journal of Geophysical Research – Atmospheres*, in prep.

McLellan, E, D Robertson, K Schilling, M Tomer, J Kostel, D Smith, and K King. 2015. “Reducing Nitrogen Export from the Corn Belt to the Gulf of Mexico: Agricultural Strategies for Remediating Hypoxia.” *Journal of the American Water Resources Association* 51(1): 263–289, <https://doi.org/10.1111/jawr.12246>

Meade, RH, and JA Moody. 2010. “Causes for the decline of suspended-sediment discharge in the Mississippi River system, 1940–2007.” *Hydrological Processes* 24(1):35–49, <https://doi.org/10.1002/hyp.7477>

- Meybeck, M. 1982. "Carbon, nitrogen, and phosphorus transport by world rivers." *American Journal of Science* 282(4): 401–450, <https://doi.org/10.2475/ajs.282.4.401>
- Milliman, JD, and RH Meade. 1983. "World-Wide Delivery of River Sediment to the Oceans." *The Journal of Geology* 91(1): 1–21, <https://doi.org/10.1086/628741>
- Rabalais, NN, RE Turner, and WJ Wiseman. 2002. "Gulf of Mexico hypoxia, aka 'The dead zone'". *Annual Review of Ecology and Systematics* 33(1): 235–263, <https://doi.org/10.1146/annurev.ecolsys.33.010802.150513>
- Turner, RE, NN Rabalais, and D Justic. 2008. "Gulf of Mexico hypoxia: Alternate states and a legacy." *Environmental Science & Technology* 42(7): 2323–2327, <https://doi.org/10.1021/es071617k>
- Tan Z, LR Leung, H Li, TK Tesfa, M Vanmaercke, J Poesen, X Zhang, H Lu, and J Hartmann. 2017. "A global data analysis for representing sediment and particulate organic carbon yield in Earth System Models." *Water Resources Research* 53(12): 10674–10700, <https://doi.org/10.1002/2017WR020806>
- Tan Z, LR Leung, H-Y Li, and T Tesfa. 2018. "Modeling Sediment Yield in Land Surface and Earth System Models: Model Comparison, Development, and Evaluation." *Journal of Advances in Modeling Earth Systems* 10(9): 2192–2213, <https://doi.org/10.1029/2017MS001270>
- Tan, Z, LR Leung, H-Y Li, T Tesfa, Q Zhu, and M Huang. 2020. "A substantial role of soil erosion in the land carbon sink and its future changes." *Global Change Biology* 26(4): 2642–2655, <https://doi.org/10.1111/gcb.14982>
- Tan, Z, LR Leung, H-Y Li, T Tesfa, Q ZXhu, X Yang, Y Liu, and M Huang. 2021. "Increased extreme rains intensify erosional nitrogen and phosphorus fluxes to the northern Gulf of Mexico in recent decades." *Environmental Research Letters* 16, 054080, <https://doi.org/10.1088/1748-9326/abf006>
- Van Meter, KJ, P Van Cappellen, and NB Basu. 2018. "Legacy nitrogen may prevent achievement of water quality goals in the Gulf of Mexico." *Science* 360(6387): 427–430, <https://doi.org/10.1126/science.aar4462>
- Valderrama-Landeros, L, and F Flores-de-Santiago. 2019. "Assessing coastal erosion and accretion trends along two contrasting subtropical rivers based on remote sensing data." *Ocean and Coastal Management* 169: 58–67, <https://doi.org/10.1016/j.ocecoaman.2018.12.006>
- Voisin, N, MI Hejazi, L Liu, TK Tesfa, H Li, M Huang, Y Liu, and LR Leung. 2013a. "One-way coupling of an integrated assessment model and a water resources model: evaluation and implications of future changes over the US Midwest." *Hydrology and Earth System Sciences* 17(11): 4555–4575, <https://doi.org/10.5194/hess-17-4555-2013>
- Voisin, N, H Li, DL Ward, M Huang, MS Wigmosta, and LR Leung. 2013b). "On an improved sub-regional water resources management representation for integration into earth system models." *Hydrology and Earth System Sciences* 17(9): 3605–3622, <https://doi.org/10.5194/hess-17-3605-2013>

Warrick, JA, AW Stevens, IM Miller, SR Harrison, AC Ritchie, and G Gelfenbaum. 2019. “World’s largest dam removal reverses coastal erosion.” *Scientific Reports* 9, 13968, <https://doi.org/10.1038/s41598-019-50387-7>

Yigzaw, W, H-Y Li, X Fang, LR Leung, N Voisin, MI Hejazi, and Y Demissie. 2019. “A multilayer reservoir thermal stratification module for earth system models.” *Journal of Advances in Modeling Earth Systems* 11(10): 3265–3283, <https://doi.org/10.1029/2019MS001632>

Yigzaw, W, H-Y Li, Y Demissie, MI Hejazi, LR Leung, N Voisin, and R Payn. 2018. “A new global reservoir geometry dataset for representing reservoirs in land surface and earth system models.” *Water Resources Research* 54(12): 10372–10386, <https://doi.org/10.1029/2017WR022040>

Zaehle, S, P Ciais, AD Friend, and V Prieur. 2011. “Carbon benefits of anthropogenic reactive nitrogen offset by nitrous oxide emissions.” *Nature Geoscience* 4: 601–605, <https://doi.org/10.1038/ngeo1207>



U.S. DEPARTMENT OF
ENERGY

Office of Science